The EMBO Journal (2005) 24, 1863–1873 | © 2005 European Molecular Biology Organization | All Rights Reserved 0261-4189/05
www.embojournal.org

THE EMBO JOURNAL

Impaired maturation of myeloid progenitors in mice lacking novel Polycomb group protein MBT-1

Satoko Arai and Toru Miyazaki*

Center for Immunology, University of Texas Southwestern Medical Center, Dallas, TX, USA

Polycomb group (PcG) proteins participate in DNA-binding complexes with gene-repressing activity, many of which have been highlighted for their involvement in hematopoiesis. We have identified a putative PcG protein, termed MBT-1, that is associated with Rnf2, an *in vivo* interactor of PcG proteins. MBT-1 structurally resembles the H-L(3)MBT protein, whose deletion is predicted to be responsible for myeloid hematopoietic malignancies. The human *MBT-1* gene is located on chromosome 6q23, a region frequently deleted in leukemia cells, and shows a transient expression spike in response to maturation-inducing stimuli in myeloid leukemia cells. *MBT-1*$^{-/-}$ myeloid progenitor cells exhibit a maturational deficiency but maintain normal proliferative activities. This results in the accumulation of immature myeloid progenitors and hence, a marked decrease of mature myeloid blood cells, causing the *MBT-1*$^{-/-}$ mice to die of anemia during a late embryonic stage. Together, we conclude that MBT-1 specifically regulates the maturational advancement of myeloid progenitor cells during transitions between two developmental stages. We also show that MBT-1 appears to influence myelopoiesis by transiently enhancing p57^{KIP2} expression levels.

The EMBO Journal (2005) **24,** 1863–1873. doi:10.1038/sj.emboj.7600654; Published online 5 May 2005
Subject Categories: development; immunology
Keywords: cyclin-dependent kinase inhibitor (CDKI); hematopoiesis; *mbt* repeat; polycomb; Rnf2

Introduction

Hematopoiesis is characterized by the differentiation of multipotent stem cells (hematopoietic stem cells; HSCs) into different progenitors that are progressively committed to restricted lineages, terminally becoming one specific type of mature blood cells (Weissman *et al*, 2001). Homeostasis of this process is maintained by the coordinated regulation of proliferation versus the maturational advancement of progenitor cells, which defines the proportion of cell populations at each specific developmental stage. Currently, hematopoietic progenitor cells are accurately classified according to their developmental potentials, as summarized in Supplementary Figure 1. Each type of progenitor harbors a specific cell surface phenotype, which is distinguished by the expression profiles of certain surface proteins such as c-kit, Sca-1, IL-7 receptor (IL-7R), CD34 and Fcγ receptor (FcγR) (Akashi *et al*, 2000a, b; Weissman *et al*, 2001).

Today, mammalian polycomb group (PcG) proteins are implicated as being involved in hematopoiesis (Raaphorst *et al*, 2001; Lessard and Sauvageau, 2003b). PcG genes were originally identified in the *Drosophila* as transcription repressor genes, and are involved in the maintenance of correct spatial and temporal expression of the homeotic genes during development in large protein complexes (Wismar, 2001). Many mammalian PcG proteins appear to play roles in hematopoiesis in a variety of fashion: for example, enhancement of lymphopoiesis via activation of proliferation (Raaphorst *et al*, 2001), control of B-cell development through histone H3 methylation and immunoglobulin heavy chain (IgH) rearrangement (Su *et al*, 2003) and generation of self-renewing HSCs (Lessard and Sauvageau, 2003a; Park *et al*, 2003). Of these, a population of PcG proteins harbor different repeats of a unique *mbt* domain, which was initially described in the *Drosophila* lethal(3)malignant brain tumor (*l(3)mbt*) protein. Although it is predicted that the *mbt* domain might possess a strong transcription-repressing activity (Boccuni *et al*, 2003), the physiological function(s) of the *mbt*-containing PcG proteins are yet unclear. Interestingly, the human homolog of the *l(3)mbt* gene (H-L(3)MBT gene) maps to chromosome 20q12, within a common deleted region associated with myeloid hematopoietic malignancies (Koga *et al*, 1999; Bench *et al*, 2000; MacGrogan *et al*, 2001; Li *et al*, 2004). This may also suggest a possible linkage of the *mbt*-containing PcG proteins and hematopoiesis.

From databases, we have newly isolated a putative PcG molecule, termed MBT-1. The MBT-1 structurally resembles the H-L(3)MBT. In addition, the human MBT-1 gene (h*MBT-1*) localizes to chromosome 6q23, one of the most frequently modified loci in some types of acute leukemia cells (Hayashi *et al*, 1990; Hirata *et al*, 1992; Offit *et al*, 1994; Merup *et al*, 1998; Sundareshan *et al*, 2003). Together, MBT-1 might also play a role in hematopoiesis. In this study, we provide evidence that MBT-1 specifically regulates the maturational advancement of myeloid progenitors during differentiation, involving the enhancement of cyclin-dependent kinase inhibitor activities.

Results

MBT-1, a new PcG gene expressed in hematopoietic progenitor cells, localized to human chromosome 6q23

We isolated MBT-1 as a putative PcG protein. Like many PcG proteins, MBT-1 contains nuclear localization signals (NLS) and a sterile alpha motif (SAM)/SPM domain, believed to function in the polymerization of proteins (Bornemann *et al*, 1996), at the C-terminus (Figure 1A). The strict localization of MBT-1 protein to the nucleus was evident by a confocal microscopic analysis of Chinese hamster ovarian carcinoma (CHO) cells transfected with a FLAG-tagged *MBT-1* gene

*Corresponding author. Center for Immunology, University of Texas Southwestern Medical Center, 6000 Harry Hines Boulevard NA7200, Dallas, TX 75390-9093, USA. Tel.: +1 214 648 7322; Fax: +1 214 648 7331; E-mail: Toru.Miyazaki@UTSouthwestern.edu

Received: 23 November 2004; accepted: 31 March 2005; published online: 5 May 2005

©2005 European Molecular Biology Organization

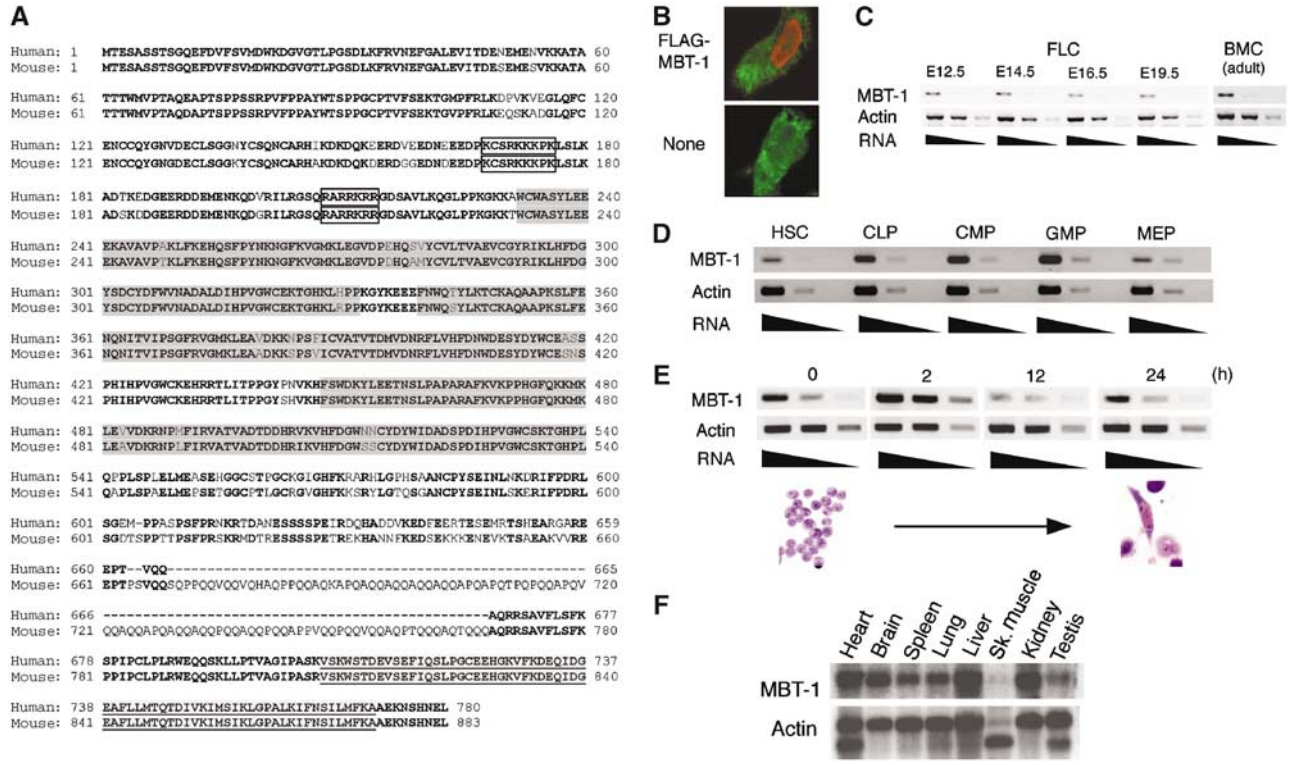

Figure 1 Identification of MBT-1. (**A**) Amino-acid sequence of human and mouse MBT. Bold, conserved amino acids between human and mouse; boxed, NLS; shadowed, the *mbt* motifs; shadowed and underlined, the SAM/SPM domain. The poly-Q domain in mouse MBT-1 is present between the *mbt*-3 and the SAM/SPM domains. (**B**) Nuclear localization of MBT-1. CHO cells were electroporated with pFLAG-MBT-1 and analyzed by confocal microscope after staining for FLAG sequence (Cy3; red signals). Cells were counterstained for Golgi/ER (green signals) by using mAb BIP/GRP78 and FITC-conjugated anti-mouse IgG Ab. Magnification, $\times 63$. (**C**) Semiquantitative RT–PCR analysis of RNA obtained from fetal liver cells (FLC) of embryos and bone marrow cells (BMC) of adult mice. The amounts of RNA are indicated by arrows. (**D**) Differential expression of the *MBT-1* gene in various stages of progenitors. At least 2×10^4 cells at each stage were sorted and RNA was assessed for expression of *MBT-1* and actin by semiquantitative RT–PCR. The amounts of RNA are indicated by arrows. PCR products were separated on an agarose gel, blotted on a membrane and hybridized with ^{32}P-labeled *MBT-1* or actin cDNA. (**E**) Transient induction and diminishment of *MBT-1* gene upon maturation. TF-1 cells were stimulated by TPA, and the *MBT-1* expression levels were kinetically analyzed by semiquantitative RT–PCR. The amounts of RNA are indicated by arrows. Morphological change of TF-1 cells into macrophage-like cells (cell photos; Giemsa staining; magnification, $\times 40$) due to differentiation started 6 h after stimulation, and was established within 24 h. Three independent experiments were performed, and the representative result is demonstrated. (**F**) Northern blotting. A 2 μg portion of polyA-RNA isolated from different tissues of adult C57BL/6 mice was separated on 1% agarose gel, blotted on a nylon membrane and hybridized with ^{32}P-labeled mouse *MBT-1* full-length cDNA or β-actin cDNA.

(Figure 1B). Similar to *l(3)mbt* (and its human homolog H-L(3)MBT), MBT-1 is characterized by three repeats of the *mbt* motif. Interestingly, the mouse homolog of MBT-1 harbors a unique glutamine-rich domain (poly-Q), which is absent in human MBT-1. This domain probably strengthens protein–protein interactions, resulting in the polymerization/aggregation of nuclear molecules, as in macrophage glutamine repeat protein-1 (GRP-1) (Cox *et al*, 1996). Other components are, however, highly conserved in human and mouse clones (Figure 1A).

Hematopoietic cells, in the fetal liver of the mouse embryo and the bone marrow of adult mouse, displayed comparable levels of *MBT-1* expression throughout development when analyzed by RT–PCR (Figure 1C). In addition, all types of hematopoietic progenitor cells in the murine fetal liver expressed the *MBT-1* gene (Figure 1D).

Next, we analyzed the expression kinetics of *MBT-1* during the differentiation of immature hematopoietic cells using a leukemia cell line. As shown in Figure 1E, in TF-1 cells (a human erythroleukemia cell line derived from myeloid progenitor cells; Kitamura *et al*, 1989), the *MBT-1* expression level significantly increased (approximately 8- to 10-fold) within 2 h in response to induction of differentiation by 2-*O*-tetradecanoylphorbol 13-acetate (TPA). It was then rapidly downregulated, and displayed the lowest level, which was even lower than the endogenous level before stimulation, during a late stage of differentiation, that is, 12 h after stimulation. Similar results were also obtained by using other leukemia cell lines such as HL-60 and KG-1 (data not shown). In addition to hematopoietic cells, *MBT-1* is expressed in multiple mouse tissues, when analyzed by Northern blotting (Figure 1F).

Embryonic lethality of MBT-1$^{-/-}$ mice due to anemia

To address the potential contribution of MBT-1 to hematopoiesis *in vivo*, we generated mice incapable of making MBT-1 (*MBT-1$^{-/-}$*), by replacing exon 15 and a part of the intron of the *MBT-1* gene with a neomycin resistance gene (neo^r) via homologous recombination in embryonic stem (ES) cells (Figure 2A). When timed pregnancies from intercross breeding of mice carrying the mutation in the heterozygous state (*MBT-1$^{+/-}$*) were analyzed, all of the *MBT-1$^{-/-}$* embryos died during a late embryonic stage (between E17.5 and E19.5) (Figure 2B). Complete lack of the *MBT-1* expression was

 ©2005 European Molecular Biology Organization

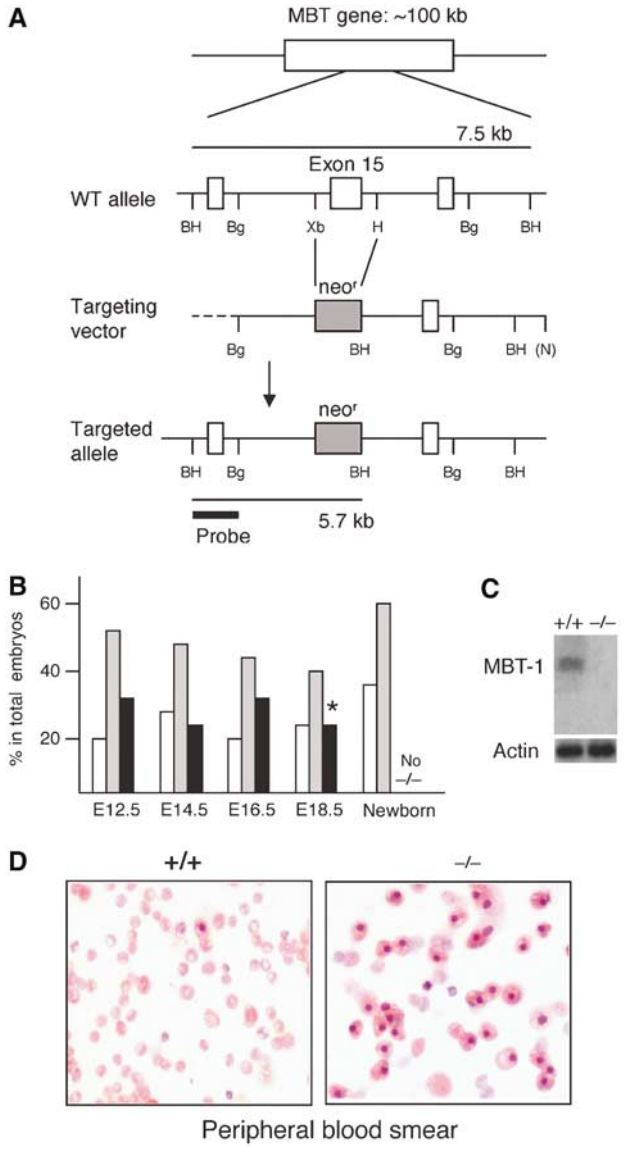

Figure 2 *MBT-1*$^{-/-}$ mice are embryonic lethal due to anemia. (**A**) Knockout strategy. Restriction maps are shown for the wild-type *MBT-1* gene locus (WT allele), targeting vector and recombinant gene locus (Targeted allele). Exons, white boxes; neo^r, shadowed box; pBluescript vector sequence, dashed line. Restriction sites: BH, *Bam*HI; Bg, *Bgl*II; Xb, *Xba*I; H, *Hin*dIII; (N), *Not*I from lambda phage sequence. Probe DNA fragment for Southern blotting is indicated, as are the 7.5- and 5.7-kb *Bam*HI hybridized fragments in wild-type and mutant DNA, respectively. (**B**) Numbers of embryos of +/+ (open boxes), +/− (shadowed boxes) and −/− (filled boxes) represented as percentages of each genotype in embryos collected from three to four timed pregnancies from +/− intercross breeding. *At E18.5, some −/− embryos were lethal. In newborns, no live −/− mice were observed. (**C**) Northern blotting. Total liver RNA from wild-type (left) or mutant (right) E14.5 embryos was analyzed by Northern blotting for *MBT-1* (upper) or actin (lower) expression. A DNA fragment of full-length mouse *MBT-1* cDNA was used as a probe. After stripping the *MBT-1* probe, ^{32}P-labeled β-actin cDNA was rehybridized on the same membrane. Neither full-length nor shorter variant RNA of *MBT-1* was detected in mutant mice. (**D**) Peripheral blood smears from +/+ or −/− embryos at E16.5 stained by Giemsa solution. In −/−, many nucleated immature erythrocytes were observed. Magnification, ×40.

confirmed by Northern blot analysis of the fetal liver RNA (Figure 2C). *MBT-1*$^{-/-}$ embryos were visibly paler than wild-type embryos. Consistent with this phenotype, the peripheral blood of *MBT-1*$^{-/-}$ embryos from a late embryonic stage (E16.5) contained a larger proportion of nucleated immature erythrocytes when compared with that of *MBT-1*$^{+/+}$ embryos at the same embryonic stage (Figure 2D). In addition, hematocrit (Ht) levels were lower in *MBT-1*$^{-/-}$ embryos ($41\pm4\%$ in *MBT-1*$^{+/+}$ versus $11\pm3\%$ in *MBT-1*$^{-/-}$ at E17.5 ($n=6$–8 for each)). These results, together with the normal development of other organs, as assessed by histological analysis (Supplementary Figure 2), suggest that the loss of MBT-1 disturbed definitive erythropoiesis, resulting in embryonic lethality of *MBT-1*$^{-/-}$ mice caused by anemia.

Inefficient maturation of MBT-1$^{-/-}$ *myeloid lineage cells*

In addition to erythrocytes, other types of mature myeloid lineage cells were also decreased in the *MBT-1*$^{-/-}$ fetal liver at a late embryonic stage (E17.5). As displayed in Figure 3A, the absolute number of granulocytes (Gr-1$^+$Mac-1$^+$) was approximately 14 times less in *MBT-1*$^{-/-}$ than in *MBT-1*$^{+/+}$ animals. Similarly, macrophages (Mac-1$^+$Gr-1$^-$) were also markedly decreased in number. However, in sharp contrast to the decrease of mature myeloid cells, the absolute numbers of the relevant upstream progenitors (megakaryocyte/erythrocyte progenitor (MEP) and granulocyte/macrophage progenitor (GMP); refer Supplementary Figure 1) were markedly increased in *MBT-1*$^{-/-}$ animals (Figure 3B). Common myeloid progenitor (CMP) cells, the upstream precursors for GMP and MEP cells, were also increased in number (Figure 3B). Similarly, the proportion of lineage markers-negative (Lin$^-$) progenitor cells in total FLCs was increased in *MBT-1*$^{-/-}$ mice than *MBT*$^{+/+}$ mice (Figure 3C). These observations strongly suggest that the maturational transition of progenitors toward mature myeloid lineage cells is defective, resulting in the accumulation of immature progenitor cells in *MBT-1*$^{-/-}$ mice. In order to assess whether the proliferative potentials of these myeloid progenitor cells were influenced in *MBT-1*$^{-/-}$ mice, we compared the incorporation of BrdU by those cells from *MBT-1*$^{+/+}$ and *MBT-1*$^{-/-}$ animals. As shown in Figure 3D, the incorporation of BrdU was essentially equivalent in *MBT-1*$^{+/+}$ and *MBT-1*$^{-/-}$ animals in each type of progenitor cells, clearly indicating that the lack of MBT-1 does not affect proliferation of the progenitor cells. In addition, the proportions of Annexin V (a marker for apoptotic cells)-positive cells in mature granulocytes and macrophages were equivalent in *MBT-1*$^{+/+}$ and *MBT-1*$^{-/-}$ fetal livers (granulocytes (Gr-1$^+$Mac-1$^+$): $5.2\pm0.4\%$ in *MBT-1*$^{+/+}$ versus $4.9\pm0.6\%$ in *MBT-1*$^{-/-}$; macrophages (Gr-1$^-$Mac-1$^+$): $8.2\pm0.6\%$ in *MBT-1*$^{+/+}$ versus $8.0\pm0.2\%$ in *MBT-1*$^{-/-}$; $n=5$ each). Therefore, decrease of mature myeloid cells in *MBT-1*$^{-/-}$ animals was not due to accelerated apoptosis of those cells.

In contrast to myeloid lineage cells, the decrease in lymphocyte numbers was less marked in *MBT-1*$^{-/-}$ animals. The proportion of B220^{high+} mature B cells in the fetal liver was slightly decreased in *MBT-1*$^{-/-}$ mice (Figure 3E), and T-cell (thymocyte) differentiation was almost comparable in mutant and wild-type mice, both in cell number and in maturation profiles (Figure 3F). Similarly, the number of common lymphoid progenitor (CLP) cells was equivalent in mutant and wild-type embryos at E17.5 (Figure 3G). In addition, no difference was observed in BrdU incorporation by CLP cells in wild-type and mutant mice (Figure 3H). Thus, MBT-1 predominantly regulates myelopoiesis.

©2005 European Molecular Biology Organization

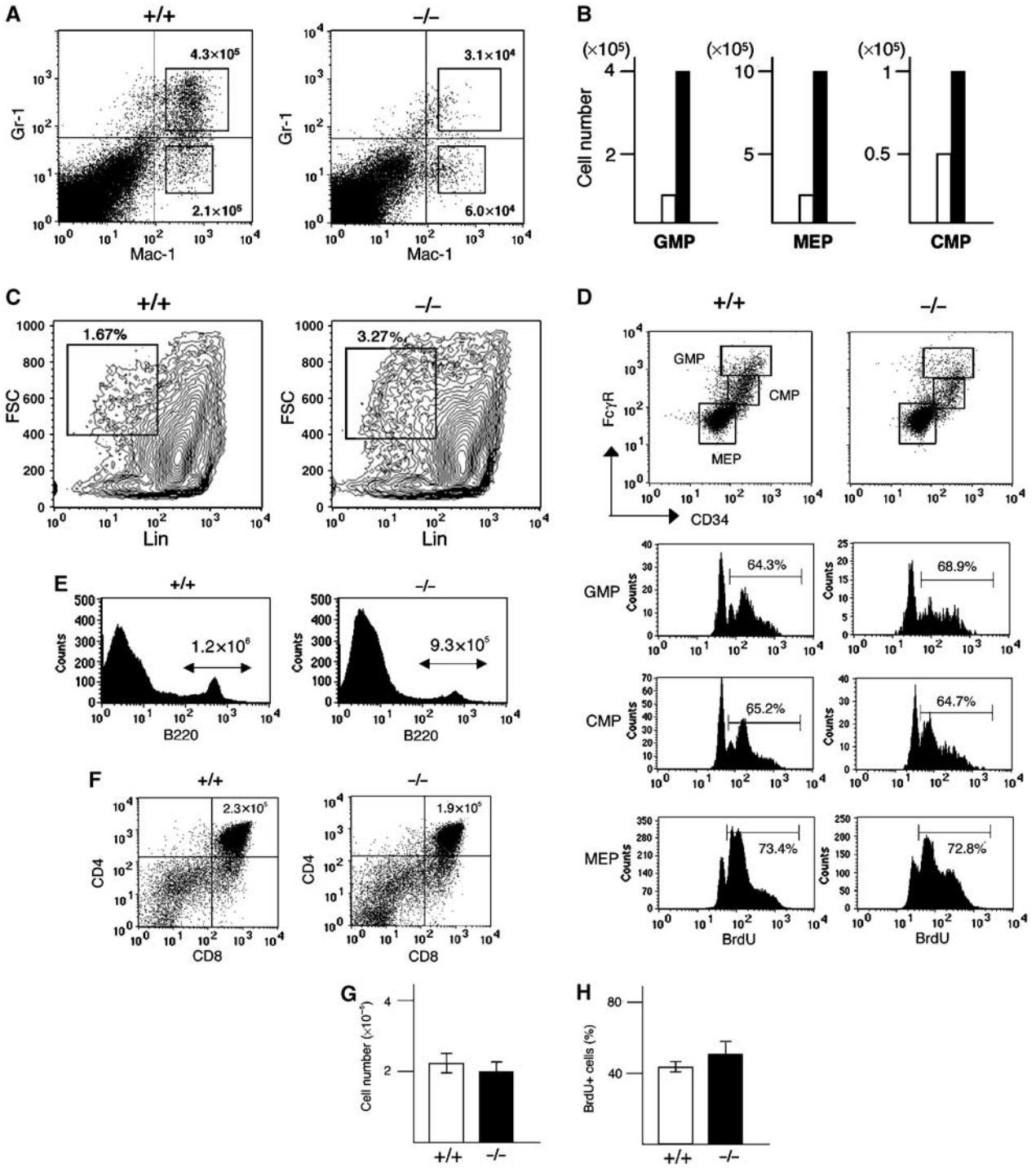

Figure 3 Deficient myelopoiesis in *MBT-1*$^{-/-}$ embryos. (**A**) Fewer mature granulocytes and macrophages in *MBT-1*$^{-/-}$ embryos. E16.5 FLCs from wild-type (+/+) or mutant (−/−) mice were stained by Gr-1 and Mac-1 Abs and analyzed using a FACSCalibure cytometer. Absolute numbers of mature granulocytes (Gr-1^{+}Mac-1^{+}) and macrophages (Gr-1^{-}Mac-1^{+}) are presented. (**B**) FLCs from +/+ and −/− at E17.5 negative for the lineage markers (Lin: CD3, B220, Ter119, DX-5, Gr-1, Mac-3) and IL-7R stained for c-kit, Sca-1, CD34 and FcγR, and analyzed by a FACSCalibure cytometer. Based on the CD34/FcγR profiles of c-kit^{+}Sca-1^{-} cells, absolute numbers for GMP, MEP and CMP were determined. Open boxes, *MBT-1*$^{+/+}$; filled boxes, *MBT-1*$^{-/-}$. In contrast to the marked reduction of mature myeloid cells, all of their immediate progenitors were increased in mutant mice. Data are representative of 4–5 mice analyzed for each genotype. (**C**) FLCs from E17.5 wild-type (+/+) or mutant (−/−) embryos stained for Lin, and analyzed by flow cytometry. The relative proportion of the Lin^{-} population (gated) is indicated by number. A total of 4–5 mice were analyzed for each genotype and the representative data are presented. (**D**) BrdU incorporation by CMP, GMP or MEP cells analyzed by flow cytometry. CD34/FcγR profiles and the gated populations are displayed. The BrdU levels in each type of progenitor cells are presented by histograms. Numbers indicate the proportions of BrdU^{+} cells. Three mice for each genotype were analyzed, and the representative data are shown. (**E**) Histograms for B220^{+} cells in E17.5 FLCs and their total numbers. (**F**) CD4/CD8 profiles and the total numbers of thymocytes from E17.5 embryos. The total numbers represent averages of 4–5 mice analyzed. (**G, H**) Total number (G) and BrdU incorporation (H) of CLP cells (Lin^{-}c-kit^{low}Sca-1^{low}IL-7R^{+}). The total numbers are averages of 3–4 embryos for each genotype analyzed.

©2005 European Molecular Biology Organization

The defect of myelopoiesis in MBT-1$^{-/-}$ mice is of cell-autonomous nature

To address whether the maturational defect of myeloid progenitor cells in *MBT-1*$^{-/-}$ mice is cell autonomous or secondary to an abnormal microenvironment, we purified *MBT-1*$^{+/+}$ or *MBT-1*$^{-/-}$ CMP cells, and differentiated them *in vitro* on irradiated OP-9 stromal feeder cells in the presence of SCF, IL-11 and Tpo. After 48 h of culture, the proportion of remaining CMP cells and the maturational status of newly developed GMP cells were analyzed, by staining the cells for CD34, FcγR, Gr-1 and Mac-1. As shown in Figure 4A, most *MBT-1*$^{+/+}$ CMP cells differentiated into either GMP or MEP cells. A large number of the newly developed *MBT-1*$^{+/+}$ GMP cells already displayed downregulation of CD34 levels, and upregulation of Gr-1 and Mac-1 maturation markers (Figure 4C, dashed lines in histograms). In contrast, many *MBT-1*$^{-/-}$ cells remained at the CMP stage, and a much lower number of GMP cells had developed (Figure 4A and B). In addition, the newly differentiated *MBT-1*$^{-/-}$ GMP cells harbored high levels of CD34 and low or negative Gr-1 and Mac-1 expression (Figure 4C, solid lines in histograms), indicating that *MBT-1*$^{-/-}$ GMP cells were less mature than *MBT-1*$^{+/+}$ GMP cells. Thus, the absence of MBT-1 disturbs the maturation of CMP cells into the GMP stage in a cell-autonomous fashion. This result was further supported by the reconstitution experiments using mutant or wild-type FLCs. At 4 weeks after the transplantation of *MBT-1*$^{+/+}$ or *MBT-1*$^{-/-}$ FLCs into lethally irradiated recipient mice, the proportion of donor-derived myeloid cells (Gr-1^{+} cells) in the peripheral blood was significantly smaller in recipient mice inoculated with mutant FLCs than those with wild-type FLCs (Figure 4D).

Interestingly, the development of MEP cells from CMP cells appeared normal in the absence of MBT-1, since both wild-type and mutant CMP cells gave rise to a comparable proportion of MEP cells after the culture (CD34^{low}FcγR^{-} cells in Figure 4A; 48% for *MBT-1*$^{+/+}$ versus 56% for *MBT-1*$^{-/-}$). Thus, the maturational defect causing anemia in *MBT-1*$^{-/-}$ mice may exist between the MEP and the mature erythrocyte stages, but not between the CMP and the MEP stages. To address this hypothesis, we performed the colony-forming cell (CFC) assay using purified MEP cells. As shown in Figure 4E, when equal numbers of *MBT-1*$^{+/+}$ or *MBT-1*$^{-/-}$ MEP cells were cultured in methylcellulose in the presence of SCF, IL-3, IL-6 and Epo for 12 days, many colonies containing large clusters of mature erythrocytes developed from *MBT-1*$^{+/+}$ MEP cells, whereas much less of these emerged from *MBT-1*$^{-/-}$ MEP cells (Figure 4F). Most of the colonies derived from *MBT-1*$^{-/-}$ MEP cells consisted of nonclustered homogenous round cells that were apparently different from mature cells (Figure 4E). These cells were c-kit^{high+}, indicating their immature status, in contrast to low or no c-kit expression on the mature cells (Figure 4G). Therefore, *MBT-1*$^{-/-}$ MEP cells cannot efficiently differentiate to mature erythrocytes, and remain at the MEP stage and continue to proliferate.

MBT-1$^{-/-}$ CMP cells require a larger number of cell divisions in order to achieve maturation to the GMP stage

When *MBT-1*$^{-/-}$ myeloid progenitors reveal inefficient maturation transition and normal proliferative activity, *MBT-1*$^{-/-}$ CMP cells may undergo more cell divisions than *MBT-1*$^{+/+}$ CMP cells prior to maturation into the GMP stage. To address this hypothesis, we directly determined the number of divisions made by *MBT-1*$^{+/+}$ or *MBT-1*$^{-/-}$ progenitor cells during the maturation between CMP and GMP stages. *MBT-1*$^{+/+}$ or *MBT-1*$^{-/-}$ CMP cells were labeled with the fluorescent dye carboxy-fluorescein diacetate, succinimidyl ester (CFDA-SE), which diffuses into cells and is inherited by daughter cells: cell division results in sequential halving of CFDA-SE fluorescence (Weston and Parish, 1990). The labeled CMP cells were differentiated *in vitro*. Thereafter, cells were stained for CD34, FcγR and Gr-1, and the CFDA-SE intensities for newly developed *MBT-1*$^{+/+}$ or *MBT-1*$^{-/-}$ GMP cells at the same maturational state (displaying the same CD34/FcγR levels) were analyzed. We estimated the numbers of cell division undergone during the period, based on the CFDA-SE levels before and after the culture (both are indicated in Figure 5A). Overall, as we predicted, *MBT-1*$^{-/-}$ cells had undergone a larger number of cell divisions than *MBT-1*$^{+/+}$ cells did before reaching the same maturation stage (Figure 5A). As an alternative analysis, the maturational states of *MBT-1*$^{+/+}$ and *MBT-1*$^{-/-}$ GMP cells (FcγR^{high}) harboring an identical CFDA-SE intensity were compared by examining Gr-1 expression. As demonstrated in Figure 5B, *MBT-1*$^{-/-}$ cells showed markedly lower levels of Gr-1 than *MBT-1*$^{-/-}$ cells did, indicating a delayed maturation for *MBT-1*$^{-/-}$ cells after an equal number of cell divisions.

Decreased p57^{KIP2} expression levels in MBT-1$^{-/-}$ FLCs

To begin to understand the molecular mechanism of how MBT-1 promotes maturation, we compared gene expression profiles of FLCs obtained from *MBT-1*$^{+/+}$ and *MBT-1*$^{-/-}$ mice by Affimetrix microarray analysis. This identified a significant reduction of the expression level of p57^{KIP2}, a KIP/CIP cdk inhibitor family member, in *MBT-1*$^{-/-}$ FLCs (MIAMExpress: accession number E-MEXP-219). This observation was also confirmed by RT–PCR (Figure 6A). In contrast to p57^{KIP2}, other cdk inhibitors, such as p21$^{WAF1/CIP1}$, p27^{KIP1} and p18^{INK4c}, showed comparable expression levels in mutant and wild-type FLCs (Figure 6A). In addition, the expression levels of various genes known to be involved in myelopoiesis such as PU.1, GATA-1, CEBP/α, AML-1, GATA-2, c-mpl, c-Myb or EpoR (Akashi *et al*, 2000a; Barreda and Belosevic, 2001; Friedman, 2002) were not altered in *MBT-1*$^{-/-}$ FLCs (data not shown). The p57^{KIP2} protein inhibits cyclins and cdks of multiple types with the greatest influence on cdk2 complexes (Yan *et al*, 1997), and p57^{KIP2}-deficient (p57$^{KIP2-/-}$) animals display a maturational delay in multiple tissues (Yan *et al*, 1997; Zhang *et al*, 1997). Hence, we hypothesized that MBT-1 may promote maturational advancement of myeloid progenitor cells by inducing cell cycle arrest preceding transition points via enhancement of p57^{KIP2} expression.

Like the *MBT-1* gene, the p57^{KIP2} level also displayed a transient expression spike during the maturation process when assessed in TF-1 cells (Figure 6B). Importantly, the levels of both *MBT-1* and p57^{KIP2} are markedly downregulated during a late stage of maturational transition (Figure 6B). This response should make the cell cycle interference via the MBT-1–p57^{KIP2} pathway restricted to the transitional period of progenitor cell maturation, and preserve normal cell proliferation after transition. Indeed, the lack of MBT-1 did not influence BrdU incorporation by all three myeloid progenitors (refer Figure 3D).

©2005 European Molecular Biology Organization

In order to test the actual involvement of $p57^{KIP2}$ in the downstream functional pathway of MBT-1, we addressed whether overexpression of $p57^{KIP2}$ via adenovirus infection would overcome the maturational deficiency in *MBT-1*$^{-/-}$ CMP cells during *in vitro* culture. As shown in Figure 6C and D, the pAd-$p57^{KIP2}$ infection significantly improved the

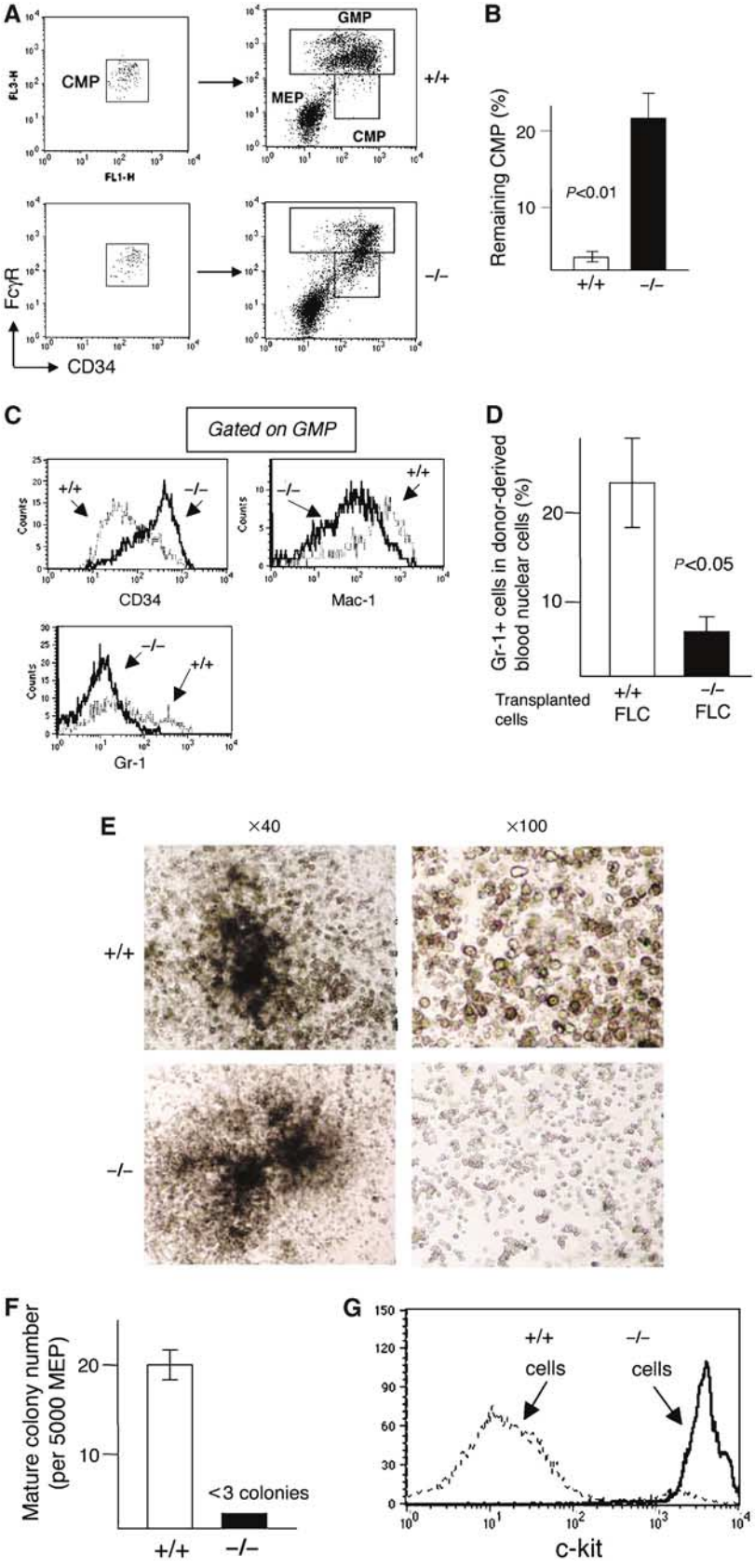

©2005 European Molecular Biology Organization

maturation of *MBT-1*$^{-/-}$ CMP cells. Hence, we conclude that the enhancement of p57^{KIP2} expression is an important mechanism for the maturation regulation of hematopoietic progenitors by MBT-1.

MBT-1 associates with Rnf2 (Ring1b)

A hallmark of PcG proteins is that they form multimeric DNA-binding complexes, consisting of both PcG and non-PcG proteins (Raaphorst *et al*, 2001; Lessard and Sauvageau, 2003a, b). In vertebra, at least two distinct types of PcG complex have been identified. The 'HPC–HPH' complex contains Bmi-1, HPH, HPC, Ring1a (also called Ring1) and Rnf2 (also called Ring1b), and appears to be involved in stable maintenance of gene silencing. The other, the 'EED–EZH' complex, consists of Eed, Ezh2 and YY1, making the 'epigenetic mark' necessary for the establishment and memory trace of the silent state (Poux *et al*, 2001; Raaphorst *et al*, 2001; Satijn *et al*, 2001; Cao *et al*, 2002; Lessard and Sauvageau, 2003a, b).

In order to address whether MBT-1 may also participate in a protein complex, we performed a two-hybrid screen using a complementary DNA library prepared from E17 mouse embryos. Up to 39 positive clones that were shown to synthesize MBT-1-binding proteins were sequenced. Of these, one clone encoded Rnf2. We confirmed the association between MBT-1 and Rnf2 in the yeast, by using the full-length cDNA fragments of *MBT-1* and *Rnf2*. As shown in Figure 7A, the yeast cells expressing both MBT-1 and Rnf2 (Figure 7A, a) survived in the absence of histidine and adenine, and revealed α-galactosidase activity (Figure 7A, a), while those producing only MBT-1 (Figure 7A, b) did not. This result confirmed the *in vivo* interaction of MBT-1 and Rnf2 in yeast cells. In agreement with this result, MBT-1 and Rnf2 co-immunoprecipitated each other in mammalian cells, when tested by using cell lysates from 293T cells transfected with tagged *MBT-1* and *Rnf2* genes (Figure 7B). Together, these results clearly identify Rnf2 as a binding partner of MBT-1.

Within the 'HPC–HPH' PcG complex, Rnf2 associates with Bmi-1 through the ring finger domain of Bmi-1, and this interaction is essential for Bmi-1's ability to mediate cell cycle control by means of the *Cdkn2a* (*Ink4a/ARF*) locus (Alkema *et al*, 1997; Jacobs *et al*, 1999; Voncken *et al*, 2003). This was also proven by a significant increase in the expression level of p16^{INK4a} in both Bmi-1$^{-/-}$ and Rnf2$^{-/-}$ cells (Park *et al*, 2003; Voncken *et al*, 2003). Based on the association of MBT-1 and Rnf2, we also assessed whether the p16^{INK4a} level may increase in the absence of MBT-1. To this end, we analyzed p16^{INK4a} mRNA expression in *MBT-1*$^{-/-}$ and *MBT-1*$^{+/+}$ FLCs by RT–PCR using several sets of primers. However, the p16^{INK4a} expression was undetectable in both types of FLCs (data not shown), demonstrating that lack of MBT-1 does not increase p16^{INK4a} expression. There was no detectable expression of p16^{INK4a} in wild-type FLCs and this is consistent with the previous work by Zindy *et al* (1997).

Discussion

In this study, the newly characterized MBT-1 represents a novel form of hematopoietic regulation: controlling the maturational advancement of myeloid progenitors at transition points without influencing their proliferative potentials, in part by transiently enhancing the expression levels of the cdk inhibitor p57^{KIP2}. The *MBT-1*$^{-/-}$ mice thus revealed accumulation of immature progenitor cells and a marked reduction of mature blood cells in the myeloid lineage, leading mice to death due to overt anemia during a late embryonic stage. The maturational defect of myeloid progenitors in *MBT-1*$^{-/-}$ mice is cell autonomous, because the inefficient maturation of purified progenitor cells is also apparent (i) *in vitro* when differentiated either on OP-9 stromal feeder cells or on methylcellulose supplemented with appropriate sets of cytokines and growth factors, and (ii) *in vivo* after being transplanted into lethally irradiated recipient mice.

The association of MBT-1 and Rnf2, together with the fact that MBT-1 structurally resembles *l(3)mbt* (and its human homolog H-L(3)MBT) and that a substantial transcription-repression activity has been proposed for the function of the *mbt* repeat (Boccuni *et al*, 2003), strongly supports the idea that MBT-1 belongs to PcG. Interestingly, the expression level of p16^{INK4a}, which is the target gene of Bmi-1, which also forms a complex with Rnf2, was not increased in *MBT-1*$^{-/-}$ cells. Thus, the fine composition of PcG complexes may differ at each target gene, in each cell type and during each developmental stage, as suggested by accumulating evidence (Strutt and Paro, 1997; Satijn and Otte, 1999; Gunster *et al*, 2001; Raaphorst *et al*, 2001; Voncken *et al*, 2003). Alternatively, an unknown PcG complex containing MBT-1 and Rnf2, which is different from the two known complexes in vertebra ('HPC–HPH' and 'EED–EZH' complexes), might exist and play a distinct role. Further studies will clarify the PcG complex containing MBT-1.

The enhancement of p57^{KIP2} expression may not be the sole machinery downstream of MBT-1, since the rescue by

Figure 4 Maturational defect of myeloid progenitor cells in *MBT-1*$^{-/-}$ mice is cell autonomous. (**A–C**) *In vitro* maturation of CMP cells. (A) A total of 5000–10 000 CMP cells sorted from E14.5 +/+ or −/− FLCs were cultured on irradiated OP-9 cells in the presence of SCF, IL-11 and Tpo. After 48 h culture, nonadherent cells were stained for CD34, FcγR, Gr-1 and Mac-1, and analyzed using a FACSCalibure cytometer. CD34/FcγR profiles of sorted CMP cells before the culture (left) and the differentiated stages after the culture (right) are presented. The remaining CMP cells and newly developed GMP cells are gated in the right panels. MEP (CD34^{low}FcγR^{-}) cells are indicated (right panels). (B) Proportions of remaining CMP cells. Data are the means of four independent experiments. The difference between wild-type cells (white box) and mutant cells (black box) was statistically significant (Mann–Whitney test; $P<0.01$). Error bar: s.e.m. (C) Histograms of CD34, Gr-1 or Mac-1 levels of GMP cells developed from CMP cells. Dashed lines, +/+; solid lines, −/−. (**D**) B6 (Ly9.1^{-}) mice were lethally irradiated (900 rad) and injected with 5×10^5 FLCs (Ly9.1^{+}) isolated from *MBT-1*$^{+/+}$ or *MBT-1*$^{-/-}$ fetal livers (E14.5). At 4 weeks after the transplantation, peripheral blood nuclear cells (PBC) were analyzed for Ly9.1^{+}-donor-derived Gr-1^{+} cells. Proportions of Gr-1^{+} cells are presented. Data are the means of five recipients for each type of FLCs. The difference was statistically significant (Mann–Whitney test; $P<0.05$). Error bar: s.e.m. (**E–G**) Deficient maturation of *MBT-1*$^{-/-}$ MEP cells into mature erythrocytes. After 12 days culture in methylcellulose, *MBT-1*$^{+/+}$ MEP cells gave rise to many colonies containing clusters of mature erythrocytes (E, upper panels) in which the cells were c-kit$^{negative\ or\ low}$ (G, dashed line in the histogram), while *MBT-1*$^{-/-}$ MEP cells remained at an immature stage forming colonies consisting of c-kit^{high+} (G, solid line in the histogram), large round cells (E; lower panels). Magnifications, ×40, ×100. (F) The number of mature colonies (means of three experiments) derived from *MBT-1*$^{+/+}$ MEP cells (open box) and *MBT-1*$^{-/-}$ MEP cells (filled box). Error bar, s.e.m. Magnifications, ×40, ×100.

©2005 European Molecular Biology Organization

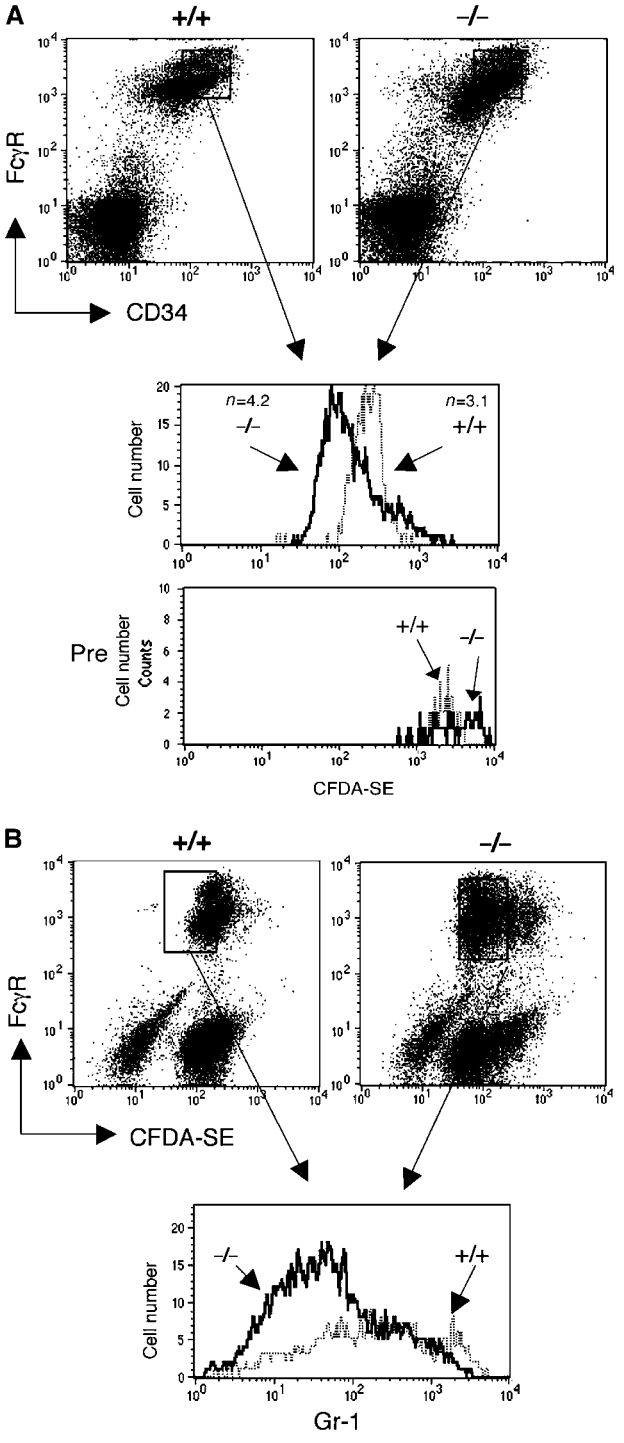

Figure 5 Increased numbers of cell divisions in *MBT-1*$^{-/-}$ progenitor cells during maturation between the CMP and GMP stages. (**A**) Upper: After 48 h culture, GMP cells exhibiting the same CD34/FcγR levels were gated and their CFDA-SE intensities are presented as histograms. Lower (indicated as Pre): CFDA-SE levels of sorted CMP cells before the culture are displayed. Dashed lines, +/+ cells; solid lines, −/− cells. Numbers of cell divisions undergone during the culture period (*n*) are indicated in the upper panels. (**B**) GMP cells harboring the same CFDA-SE intensity were gated, and their Gr-1 expression levels are displayed as histograms. Dashed lines, +/+ cells; solid lines, −/− cells.

p57^{KIP2} overexpression was not as complete as to recover the differentiation potency in mutant cells to that in wild-type cells (Figure 6C). This may also be consistent with the fact

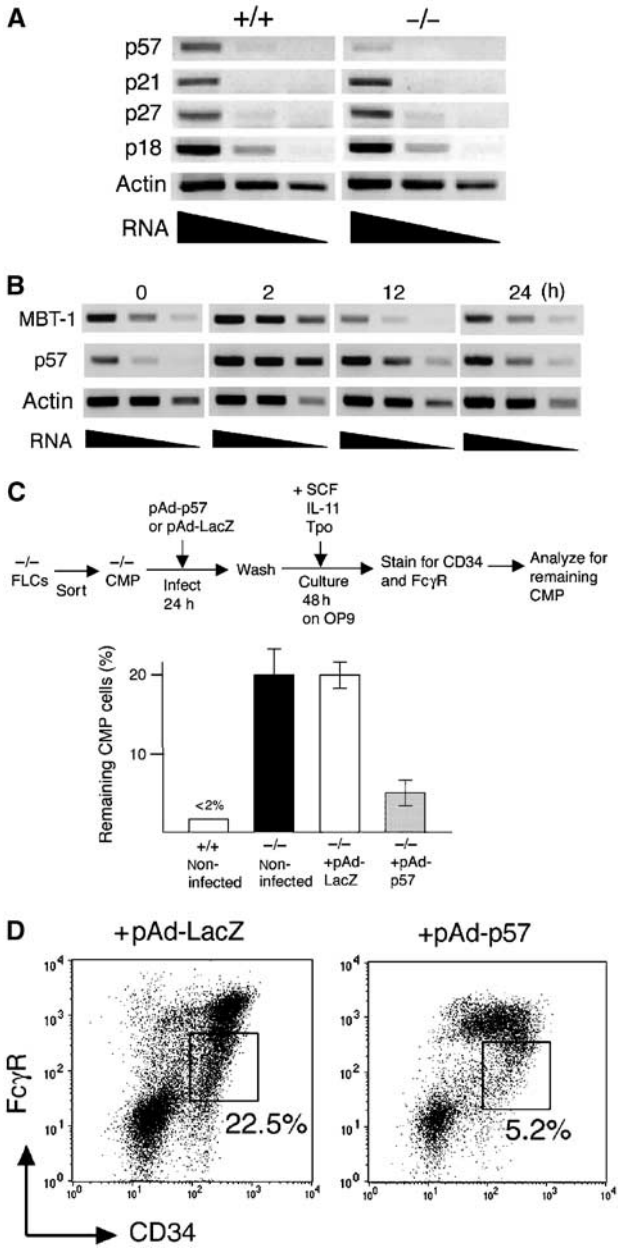

Figure 6 Decreased p57^{KIP2} expression in *MBT-1*$^{-/-}$ FLCs. (**A**) Semiquantitative RT–PCR analysis of RNA obtained from wild-type (+/+) and mutant (−/−) FLCs (E14.5) for p57^{KIP2}, p21$^{WAF1/CIP1}$, p27^{KIP1}, p18^{INK4c} (presented as p57, p21, p27, p18, respectively) and β-actin. The amounts of RNA are indicated by arrows. (**B**) Kinetics of p57^{KIP2} expression induction in response to TPA in TF-1 cells. TF-1 cells were stimulated by TPA, and the p57^{KIP2} and *MBT-1* expression levels were kinetically analyzed (0, 2, 12 and 24 h after stimulation) by semiquantitative RT–PCR. (**C**) CMP cells sorted from FLCs of E14.5 *MBT-1*$^{-/-}$ embryos, and infected either with pAd-p57 or pAd-LacZ (encoding p57^{KIP2} or LacZ, respectively). After the infection, cells were cultured *in vitro* for 48 h as described in Figure 4 legend. Thereafter, the cells were restained with CD34 and FcγR. The proportions of remaining CMP cells are presented. In wild-type cells, almost no CMP cells remained after 48 h. In noninfected mutant cells, a significant proportion of CMP cells were detected. pAd-LacZ-infected mutant cells showed an equivalent proportion of remaining CMP cells to that of noninfected mutant cells, while pAd-p57-infected mutant cells (shadowed box) showed a remarkable reduction in the remaining CMP cell proportion. (**D**) CD34/FcγR profiles of post-48-h-culture *MBT-1*$^{-/-}$ cells infected with pAd-p57 (right) or the control pAd-LacZ (left). The proportions of remaining CMP cells are indicated by numbers.

©2005 European Molecular Biology Organization

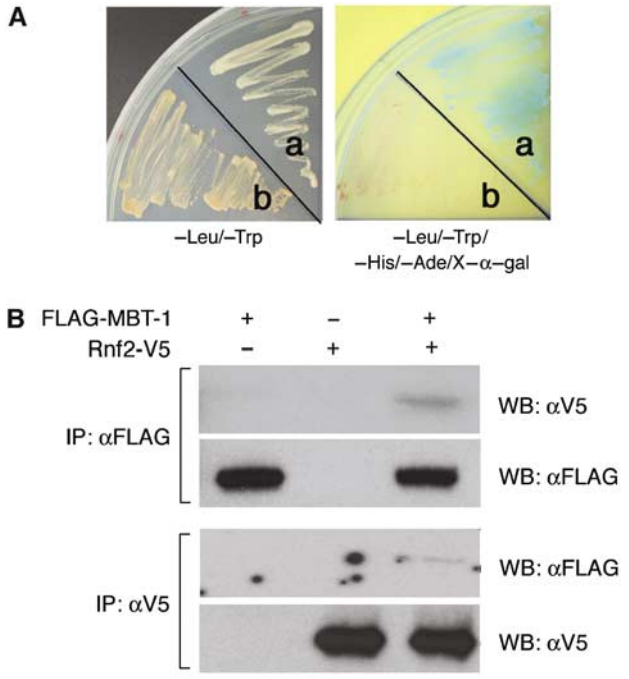

Figure 7 MBT-1 associates with Rnf2. (**A**) MBT-1 associates with Rnf2 in yeast cells. A full-length *MBT-1* cDNA fragment was subcloned into the pGBKT7 yeast expression vector, which results in expression of a fusion protein of MBT-1 and GAL4 DNA-binding domain. On the other hand, the full-length *Rnf2* cDNA fragment was cloned into the pGADT7 vector to produce a fusion protein of Rnf2 and GAL4-activating domain. Resulting plasmids were transformed into the yeast cell line AH109 harboring the reporter genes for *ADE2*, *HIS3* and *MEL1* that are under the regulation of GAL4 upstream activating sequences (UASs). The pGBKT7-containing AH109 cells can grow in the absence of tryptophan (Trp), while the pGADT7 allows AH109 cells to survive without leucine (Leu). When MBT-1 and Rnf2 associate in AH109 cells, the three reporter genes are expressed, thus allowing the cells to grow on a selective media plate lacking histidine (His) and adenine (Ade), as well as to express α-galactosidase activity. AH109 cells were transformed with (a) pGBKT7-*MBT-1* and pGADT7-*Rnf2*, or (b) pGBKT7-*MBT-1* and pGADT7-vector (without the *Rnf2* sequence). Both transformants survived on a −Leu/−Trp media plate (left), but only (a) grew and revealed α-galactosidase activity on a −Leu/−Trp/−His/−Ade/X-α-gal media plate (right). (**B**) Co-immunoprecipitation. Both or either of FLAG-tagged MBT-1 and V5-tagged Rnf2 were expressed in 293T human kidney cells. Cell lysates were immunoprecipitated by using either anti-FLAG or anti-V5 antibody conjugated with agarose beads. Precipitants were separated by SDS–PAGE, blotted on a membrane and specific signals were detected by Western blotting. IP: immunoprecipitation; WB: Western blotting.

that $p57^{KIP2-/-}$ mice are not embryonic lethal (Yan *et al*, 1997; Zhang *et al*, 1997), implying that $p57^{KIP2-/-}$ mice may not harbor, if any, as striking a deficiency in erythropoiesis during embryonic stages as do *MBT-1*$^{-/-}$ mice, although a detailed analysis of hematopoiesis has not yet been reported (Yan *et al*, 1997; Zhang *et al*, 1997). The putative $p57^{KIP2}$-independent pathway(s) for maturational regulation by MBT-1 is an area open to further clarification. Since PcG proteins are gene repressors, the enhancement of $p57^{KIP2}$ gene expression by MBT-1 is intriguing. Thus, it is possible that suppression of certain gene(s) by MBT-1 may consequently result in upregulation of $p57^{KIP2}$ expression. Further efforts are required to identify the direct target genes of MBT-1.

The function of MBT-1 is unique among the many PcG proteins involved in hematopoiesis, since their roles so far have been apparent in the regulation of proliferation of immature and/or mature lymphoid lineage cells (Raaphorst *et al*, 2001; Lessard and Sauvageau, 2003b). Interestingly, however, the regulation of maturation by MBT-1 and the proliferative control exerted by certain PcG proteins employ a similar mechanistic pathway: regulation of the expression of cdk inhibitors. For example, Bmi-1 suppresses the expression of the cdk inhibitors $p16^{INK4a}$ and $p19^{ARF}$, hence supporting the proliferation of HSCs and lymphocyte progenitors (Jacobs *et al*, 1999; Lessard and Sauvageau, 2003a; Park *et al*, 2003). Likewise, a different PcG member mel-18 also diminishes the $p16^{INK4a}$ expression and augments proliferation of T- and B-lymphocyte lineage cells (Akasaka *et al*, 1997; Jacobs *et al*, 1999). Hence, the expression of cdk inhibitors appears to be differentially regulated by nuclear factors during the maturation and proliferation of various hematopoietic lineage cells.

Another important molecular characteristic of MBT-1 is its transient alteration in expression levels at cell maturational transition points: immediate upregulation followed by rapid downregulation, upon maturation-inducing stimuli. This response may contribute to restricting the cell cycle arrest mediated by the MBT-1–$p57^{KIP2}$ pathway during the maturational transition, which allows cells to maintain a normal proliferative potential at the subsequent developmental stage. Whether this expression kinetics of *MBT-1* gene is also observed during the maturation of primary hematopoietic progenitors, and the mechanism for such kinetic regulation of *MBT-1* gene expression, will require further investigations.

MBT-1$^{-/-}$ myeloid progenitor cells reveal deficiencies in maturational advancement, but this blockade was partial in two aspects. First, some *MBT-1*$^{-/-}$ CMP cells attain a leaky differentiation to the GMP stage, although they had undergone increased numbers of cell divisions during this maturation process. Second, despite the *MBT-1* mRNA expression in all types of progenitors including CLP cells, lymphopoiesis is not affected in *MBT-1*$^{-/-}$ mice. Similarly, maturation of CMP cells to the MEP stage appears normal. This incomplete phenotype of *MBT-1*$^{-/-}$ cells may be explained by functional redundancy with other MBT-1-like molecules that are also expressed in hematopoietic progenitors. Indeed, several sequences displaying similarities with MBT-1 possessing *mbt* repeats, including H-L(3)MBT, have been published (Koga *et al*, 1999; Bench *et al*, 2000, 2001; Usui *et al*, 2000; MacGrogan *et al*, 2001; Wismar, 2001; Li *et al*, 2004) or have appeared in databases, although their functions are still unknown. In fact, we found that some of these molecules have differential expression in hematopoietic progenitor cells, as assessed by RT–PCR (data not shown). Their functional understanding will help to evaluate the possible redundancy in these MBT-1-like molecules.

Although the identification and characterization of MBT-1 has provided novel insights into the regulation of hematopoiesis, deletion of MBT-1 did not solely induce leukemia. However, the phenotype of MBT-1$^{-/-}$ mice, which is characterized by accumulation of myeloid progenitor cells, might suggest a possible role of MBT-1 dysfunction in development of preleukemia. Identification of (specific) modifications of the *MBT-1* gene in a large-scale screening of leukemia cells from patients will be necessary to further assess the putative correlation of leukemogenesis and MBT-1 dysfunction.

©2005 European Molecular Biology Organization

Materials and methods

Isolation of the MBT-1 gene

The human *MBT-1* gene (appearing as KIAA1798 or L(3)MBT-like 3 in the database with accession number XM_027074) was isolated from a database. The mouse *MBT-1* clone was isolated by BLAST analysis of the mouse EST clones (accession number NM_172787). Both human and mouse *MBT-1* cDNA clones were purified from cDNA libraries generated from human or mouse bone marrow cells using cDNA fragments as probes. These probes were amplified by RT–PCR from human or mouse bone marrow RNA using primers generated based on the database sequence of mouse or human *MBT-1* (primer sequences will appear in the 'Primer' section).

Transfection and confocal microscopic analysis

The precise procedure is available online.

Generation of MBT-1$^{-/-}$ mice

The *MBT-1*$^{-/-}$ mice were generated via homologous recombination in ES cells. The detailed procedure is available online.

Serological reagents and flow cytometry

All antibodies were purchased from BD Pharmingen or eBioscience. Details are available online.

In vitro and in vivo differentiation of progenitor cells

The *in vitro* maturation of CMP or MEP cells and their analysis were performed mainly according to the previous reports by Akashi *et al* (2000b) and Traver *et al* (2001). The precise procedures are available online. For reconstitution experiments, B6 (Ly9.1^{-}) mice were lethally irradiated (900 rad) and injected with 5×10^5 FLCs (Ly9.1^{+}) isolated from *MBT-1*$^{+/+}$ or *MBT-1*$^{-/-}$ fetal livers (E14.5). At 4 weeks after the transplantation, peripheral blood cells were analyzed for Ly9.1^{+}-donor-derived Gr-1^{+} cells. Cytokines and growth factors were purchased from R&D Systems.

BrdU-incorporation assay

FLCs were incubated in IMDM (containing FBS at 10%) at 2×10^6 cells/ml in the presence of 10 μM BrdU at 37°C for 30 min. After extensive washes with PBS, cells were prestained for PE-FcγR. This procedure also avoids non-antigen-specific binding of immunoglobulins to the Fcγ receptors expressed on the progenitor cells. Thereafter, both Lin^{+} and Sca-1^{+} cells were depleted by using MACS columns (Milteny Biotec) along with Lineage Cell Depletion kit (Milteny Biotec) and Anti-Sca-1 Microbeads (Milteny Biotec). Negative fractions were surface stained for APC-c-kit, PerCP-CD34 and PE-FcγR. Cells were then fixed, permeabilized and treated with DNase, followed by staining for BrdU by using the BrdU (FITC) Flow Kit (BD Bioscience). Cells were analyzed using the FACSCalibure cytometer (Becton Dickinson) for BrdU^{+} cells in each type of myeloid progenitors.

CFDA-SE labeling and cell division analysis

Approximately 5000 CMP cells sorted from E14.5 *MBT-1*$^{+/+}$ or *MBT-1*$^{-/-}$ FLCs were labeled with CFDA-SE by incubating the cells in the presence of 0.8 μM CFDA-SE for 15 min. After an extensive wash, cells were cultured on irradiated OP-9 cells in the presence of mouse SCF (10 ng/ml), mouse IL-11 (10 ng/ml) and mouse Tpo (10 ng/ml) for 48 h. Thereafter, nonadherent cells were stained for CD34, FcγR and Gr-1, and analyzed using a FACSCalibure cytometer. The number (n) of cell division undergone during the culture period was estimated as $n = \log 2$(CFDA-SE intensity before the culture/CFDA-SE intensity after the culture).

Adenovirus infection and in vitro differentiation of progenitor cells

The adenovirus vectors used in this work were created by using the pAd/CMV/V5-DEST Gateway system (Invitrogen) and either a LacZ sequence or mouse cDNA of p57^{KIP2}. The procedures of virus infection, cell maturation and cell analysis are available online.

Analysis of the kinetics of gene expression upon maturation induction

TF-1 cells were stimulated by 100 nM TPA supplemented in the culture medium. At 0, 2, 12 and 24 h after TPA-induced maturation, cells were harvested to isolate RNA. Expression levels of human *MBT-1*, p57^{KIP2} and actin were analyzed by semiquantitative RT–PCR. PCR products were separated on an agarose gel. The same procedures were applied when HL-60 and KG-1 cells were used.

Yeast two-hybrid screening

Yeast two-hybrid assay was performed using MATCHMAKER GAL4 Two-hybrid system 3 (BD Biosciences). The precise procedure is available online.

Immunoprecipitation

The precise procedure is available online.

Primers

Primer sequences used for RT–PCR in this work are available online.

Microarray analysis

Microarray analyses were performed by using total RNA (5 μg/experiment required) and mainly Affymetrix chips at the Microarray core facility at the University of Texas Southwestern Medical Center at Dallas.

Supplementary data

Supplementary data are available at *The EMBO Journal* Online.

Acknowledgements

We thank Dr J Richardson (Dallas) and the histology core facility (Pathology, UT-Southwestern) for histology; Dr S Kaminogawa (Tokyo) for insightful discussion; the flow cytometry core facility (Pathology, UT-Southwestern) for cell sorting; Microarray core facility (UT-Southwestern) for microarray analysis; and S Subramanian and G Westerfield for help in preparing manuscript. TM is supported by grants from NIH (RO1-AI050948A2), JDRF (#1-2001-581), ALF, PAF and HHMI. None of the authors have any financial interest related to this work.

References

Akasaka T, Tsuji K, Kawahira H, Kanno M, Harigaya K, Hu L, Ebihara Y, Nakahata T, Tetsu O, Taniguchi M, Koseki H (1997) The role of mel-18, a mammalian Polycomb group gene, during IL-7-dependent proliferation of lymphocyte precursors. *Immunity* **7:** 135–146

Akashi K, Reya T, Dalma-Weiszhausz D, Weissman IL (2000a) Lymphoid precursors. *Curr Opin Immunol* **12:** 144–150

Akashi K, Traver D, Miyamoto T, Weissman IL (2000b) A clonogenic common myeloid progenitor that gives rise to all myeloid lineages. *Nature* **404:** 193–197

Alkema MJ, Jacobs H, van Lohuizen M, Berns A (1997) Pertubation of B and T cell development and predisposition to lymphomagenesis in Emu Bmi1 transgenic mice require the Bmi1 RING finger. *Oncogene* **15:** 899–910

Barreda DR, Belosevic M (2001) Transcriptional regulation of hemopoiesis. *Dev Comp Immunol* **25:** 763–789

Bench AJ, Cross NC, Huntly BJ, Nacheva EP, Green AR (2001) Myeloproliferative disorders. *Best Pract Res Clin Haematol* **14:** 531–551

Bench AJ, Nacheva EP, Hood TL, Holden JL, French L, Swanton S, Champion KM, Li J, Whittaker P, Stavrides G, Hunt AR, Huntly BJ, Campbell LJ, Bentley DR, Deloukas P, Green AR, UK Cancer Cytogenetics Group (UKCCG) (2000) Chromosome 20 deletions in myeloid malignancies: reduction of the common deleted region, generation of a PAC/BAC contig and identification of candidate genes. *Oncogene* **19:** 3902–3913

Boccuni P, MacGrogan D, Scandura JM, Nimer SD (2003) The human L(3)MBT polycomb group protein is a transcriptional

 ©2005 European Molecular Biology Organization

repressor and interacts physically and functionally with TEL (ETV6). *J Biol Chem* **278:** 15412–15420

Bornemann D, Miller E, Simon J (1996) The *Drosophila* Polycomb group gene Sex comb on midleg (Scm) encodes a zinc finger protein with similarity to polyhomeotic protein. *Development* **122:** 1621–1630

Cao R, Wang L, Wang H, Xia L, Erdjument-Bromage H, Tempst P, Jones RS, Zhang Y (2002) Role of histone H3 lysine 27 methylation in Polycomb-group silencing. *Science* **298:** 1039–1043

Cox GW, Taylor LS, Willis JD, Melillo G, White III RL, Anderson SK, Lin JJ (1996) Molecular cloning and characterization of a novel mouse macrophage gene that encodes a nuclear protein comprising polyglutamine repeats and interspersing histidines. *J Biol Chem* **271:** 25515–25523

Friedman AD (2002) Transcriptional regulation of myelopoiesis. *Int J Hematol* **75:** 466–472

Gunster MJ, Raaphorst FM, Hamer KM, den Blaauwen JL, Fieret E, Meijer CJ, Otte AP (2001) Differential expression of human Polycomb group proteins in various tissues and cell types. *J Cell Biochem* **81** (S36)**:** 129–143

Hayashi Y, Raimondi SC, Look AT, Behm FG, Kitchingman GR, Pui CH, Rivera GK, Williams DL (1990) Abnormalities of the long arm of chromosome 6 in childhood acute lymphoblastic leukemia. *Blood* **76:** 1626–1630

Hirata J, Abe Y, Taguchi F, Takatsuki H, Nishimura J, Nawata H (1992) Deletion of chromosome 6q in two cases of acute myeloblastic leukemia and a review of the literature. *Cancer Genet Cytogenet* **58:** 181–185

Jacobs JJ, Kieboom K, Marino S, DePinho RA, van Lohuizen M (1999) The oncogene and Polycomb-group gene bmi-1 regulates cell proliferation and senescence through the ink4a locus. *Nature* **397:** 164–168

Kitamura T, Tojo A, Kuwaki T, Chiba S, Miyazono K, Urabe A, Takaku F (1989) Identification and analysis of human erythropoietin receptors on a factor-dependent cell line, TF-1. *Blood* **73:** 375–380

Koga H, Matsui S, Hirota T, Takebayashi S, Okumura K, Saya H (1999) A human homolog of *Drosophila* lethal(3)malignant brain tumor (l(3)mbt) protein associates with condensed mitotic chromosomes. *Oncogene* **18:** 3799–3809

Lessard J, Sauvageau G (2003a) Bmi-1 determines the proliferative capacity of normal and leukaemic stem cells. *Nature* **423:** 255–260

Lessard J, Sauvageau G (2003b) Polycomb group genes as epigenetic regulators of normal and leukemic hemopoiesis. *Exp Hematol* **31:** 567–585

Li J, Bench AJ, Vassiliou GS, Fourouclas N, Ferguson-Smith AC, Green AR (2004) Imprinting of the human L3MBTL gene, a polycomb family member located in a region of chromosome 20 deleted in human myeloid malignancies. *Proc Natl Acad Sci USA* **101:** 7341–7346

MacGrogan D, Alvarez S, DeBlasio T, Jhanwar SC, Nimer SD (2001) Identification of candidate genes on chromosome band 20q12 by physical mapping of translocation breakpoints found in myeloid leukemia cell lines. *Oncogene* **20:** 4150–4160

Merup M, Moreno TC, Heyman M, Ronnberg K, Grander D, Detlofsson R, Rasool O, Liu Y, Soderhall S, Juliusson G, Gahrton G, Einhorn S (1998) 6q deletions in acute lymphoblastic leukemia and non-Hodgkin's lymphomas. *Blood* **91:** 3397–3400

Offit K, Louie DC, Parsa NZ, Filippa D, Gangi M, Siebert R, Chaganti RS (1994) Clinical and morphologic features of B-cell small lymphocytic lymphoma with del(6)(q21q23). *Blood* **83:** 2611–2618

Park IK, Qian D, Kiel M, Becker MW, Pihalja M, Weissman IL, Morrison SJ, Clarke MF (2003) Bmi-1 is required for maintenance of adult self-renewing haematopoietic stem cells. *Nature* **423:** 302–305

Poux S, Melfi R, Pirrotta V (2001) Establishment of Polycomb silencing requires a transient interaction between PC and ESC. *Genes Dev* **15:** 2509–2514

Raaphorst FM, Otte AP, Meijer CJ (2001) Polycomb-group genes as regulators of mammalian lymphopoiesis. *Trends Immunol* **22:** 682–690

Satijn DP, Hamer KM, den Blaauwen J, Otte AP (2001) The polycomb group protein EED interacts with YY1, and both proteins induce neural tissue in *Xenopus* embryos. *Mol Cell Biol* **21:** 1360–1369

Satijn DP, Otte AP (1999) Polycomb group protein complexes: do different complexes regulate distinct target genes? *Biochim Biophys Acta* **1447:** 1–16

Strutt H, Paro R (1997) The polycomb group protein complex of *Drosophila melanogaster* has different compositions at different target genes. *Mol Cell Biol* **17:** 6773–6783

Su IH, Basavaraj A, Krutchinsky AN, Hobert O, Ullrich A, Chait BT, Tarakhovsky A (2003) Ezh2 controls B cell development through histone H3 methylation and Igh rearrangement. *Nat Immunol* **4:** 124–131

Sundareshan TS, Prabhash K, Bapsy PP (2003) Deletion of 6q23 as sole abnormality in acute myelocytic leukemia. *Cancer Genet Cytogenet* **143:** 87–88

Traver D, Miyamoto T, Christensen J, Iwasaki-Arai J, Akashi K, Weissman IL (2001) Fetal liver myelopoiesis occurs through distinct, prospectively isolatable progenitor subsets. *Blood* **98:** 627–635

Usui H, Ichikawa T, Kobayashi K, Kumanishi T (2000) Cloning of a novel murine gene Sfmbt, Scm-related gene containing four mbt domains, structurally belonging to the Polycomb group of genes. *Gene* **248:** 127–135

Voncken JW, Roelen BA, Roefs M, de Vries S, Verhoeven E, Marino S, Deschamps J, van Lohuizen M (2003) Rnf2 (Ring1b) deficiency causes gastrulation arrest and cell cycle inhibition. *Proc Natl Acad Sci USA* **100:** 2468–2473

Weissman IL, Anderson DJ, Gage F (2001) Stem and progenitor cells: origins, phenotypes, lineage commitments, and transdifferentiations. *Annu Rev Cell Dev Biol* **17:** 387–403

Weston SA, Parish CR (1990) New fluorescent dyes for lymphocyte migration studies. Analysis by flow cytometry and fluorescence microscopy. *J Immunol Methods* **133:** 87–97

Wismar J (2001) Molecular characterization of h-l(3)mbt-like: a new member of the human mbt family. *FEBS Lett* **507:** 119–121

Yan Y, Frisen J, Lee MH, Massague J, Barbacid M (1997) Ablation of the CDK inhibitor p57Kip2 results in increased apoptosis and delayed differentiation during mouse development. *Genes Dev* **11:** 973–983

Zhang P, Liegeois NJ, Wong C, Finegold M, Hou H, Thompson JC, Silverman A, Harper JW, DePinho RA, Elledge SJ (1997) Altered cell differentiation and proliferation in mice lacking p57KIP2 indicates a role in Beckwith–Wiedemann syndrome. *Nature* **387:** 151–158

Zindy F, Quelle DE, Roussel MF, Sherr CJ (1997) Expression of the p16INK4a tumor suppressor versus other INK4 family members during mouse development and aging. *Oncogene* **15:** 203–211

©2005 European Molecular Biology Organization